Eur. Phys. J. C (2023) 83:415
https://doi.org/10.1140/epjc/s10052-023-11592-x

THE EUROPEAN PHYSICAL JOURNAL C

Regular Article - Theoretical Physics

Hot spot model of nucleon and double parton scattering

B. Blok[1,a], **R. Segev**[1], **M. Strikman**[2]

[1] Department of Physics, Technion-Israel Institute of Technology, Haifa, Israel
[2] Physics Department, Penn State University, University Park, PA, USA

Received: 20 April 2023 / Accepted: 4 May 2023 / Published online: 17 May 2023

Abstract We calculate the rate of double parton scattering (DPS) in proton-proton collisions in the framework of the recently proposed hot spot model of the nucleon structure. The resulting rate, especially for the case of three hot spots, is compared with the current experimental data on DPS at the LHC.

1 Introduction

The 3D structure of nucleons has been attracting attention at least since discovery of quarks. For a single parton distributions factorization theorems have allowed to investigate longitudinal momentum plus transverse coordinate single parton distributions (Generalized parton distributions) This is one of the central topics that will be studied in the future EIC collider to be built at Brookhaven National Laboratory [1].

Probing correlations between the partons requires more complicated tools like four jet production, for a review see for example Ref. [2].

The nonperturbative correlations were considered in the constituent quark model to explain the success of the additive quark model, for a review see Ref. [3]. Small size (hot spot) correlations generated by the QCD evolution were introduced in Ref. [4]. Recently the multi hot spot model of nucleon was introduced in [5–7]. The parameters of the model were fixed by fitting the cross section of reaction $\gamma p \to J/\psi + gap + Y$ within the model [5] which assumes that fluctuations of the gluon field at a wide range of momentum transfer satisfy the Good Walker relation [8], for a recent review of conditions of applicability of the Good–Walker model see [9].

In the last decade a lot of progress, both theoretical [10–24] and experimental [25,26] has been made in our understanding of the double-parton scattering (DPS) which are sensitive to parton-parton correlations in transverse (relative to the. hadron high momentum) plan.

The DPS cross section is usually characterized by the so called effective cross section defined as

$$\sigma_{DPS} = \frac{\sigma_1 \sigma_2}{\sigma_{\rm eff}}, \tag{1}$$

where σ_{DPS} is the cross-section of the DPS process, σ_1 and σ_2 are the cross-sections of the individual hard partonic interactions, while $\sigma_{\rm eff}$ depends heavily on the inner structure of the colliding hadrons.

In this work we will use the hot-spot model with the parameters found in Refs. [6,7] to calculate $\sigma_{\rm eff}$.

We demonstrate that $\sigma_{\rm eff}$ strongly depends on the parameters of the hot spot model. The authors of [6,7] identify two sets of parameters compatible with DIS and their model of rapidity gap processes for $N_q = 3$ and Variable N_q hot spots respectively.

For the set with variable N_q we find $\sigma_{\rm eff} \approx 17$ mb, and for the set with $N_q \equiv 3$ we get $\sigma_{\rm eff} \approx 10.5$ mb.

The experimental data for $\sigma_{\rm eff}$ are $\approx 13 \pm 3$ mb or 15 ± 5 mb for 4 jet processes depending on the measurement [25–29]. This experimental data are however available at moderate values of $Q \sim 20$ GeV and higher. The inverse evolution using DGLAP along the lines of [16–18] leads to $\sigma_{\rm eff}$ of order 20–35 mb at low scales of order GeV where hot spot model is usually formulated. We see the tension between experimental data on DPS and the DPS cross section calculated in the hot spot model, especially for $N_q = 3$ case, which is substantially higher than the experimental one, provided the QCD evolution of $\sigma_{\rm eff}$ is taken into account (see Sect. 6 for details).

This paper is organized as follows. Section 2 we review the mean-field approach to MPI and in Sect. 3 we review the details of the hot spots model. In Sect. 4 we calculate the effective cross-section using the hot spots model. In Sect. 5 we summarize the hot spot model values of effective cross section for different best fits of hot spot model parameters,

[a] e-mail: blok@physics.technion.ac.il (corresponding author)

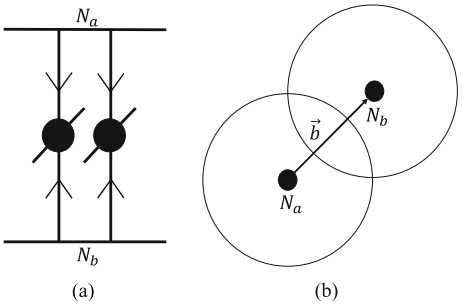

Fig. 1 **a** Parton model contribution to double parton scattering of two nucleons; **b** collision of two nucleons at the impact parameter b

and in Sect. 6 we compare these values with experimental data on DPS. In Sect. 7 we present the conclusions.

2 The mean-field approach to MPI

The hot spot model is formulated in the region of relatively small Q^2, where one can neglect the DGLAP evolution. Hence we can use the parton model to calculate the DPS cross sections.

Recall that in the parton model approach the DPS cross section is expressed through convolution of two particle generalized parton distributions ${}_2GPD$ s [13].

$$\frac{1}{\sigma_{\text{eff}}} = \frac{\int \frac{d^2\Delta}{(2\pi)^2} {}_2G(x_1, x_2, Q_1^2, Q_2^2, \Delta) {}_2G(x_3, x_4, Q_1^2, Q_2^2, \Delta)}{f(x_1, Q_1^2) f(x_2, Q_2^2) f(x_3, Q_3^2) f(x_4, Q_4^2)}. \tag{2}$$

Here $\vec{\Delta}$ is the momentum conjugate to the transverse distance between two partons participating in the DPS process (see Fig. 1).

In the mean field approximation, that is valid at small transverse scales of order several GeV and small x [13], one can prove that the two particle GPDs factorize:

$${}_2G(x_1, x_2, Q_1^2, Q_2^2, \Delta) =_1 G(x_1, Q_1^2, \Delta) {}_1G(x_1, Q_1^2, \Delta), \tag{3}$$

where ${}_1G$ are the conventional one particle GPD [30,31]. The latter in the mean field approximation can be written as

$${}_1G(x_1, Q_1^2, \Delta) = f(x_1, Q_1^2) F_{2g}(\Delta, x_1), \tag{4}$$

where F_{2g} is called a two gluon formfactor and only weakly depends on x and Q^2.

In the coordinate space we have

$$\begin{aligned} {}_1G(x, Q^2, \vec{r}) &= f(x, Q^2)\rho(\vec{r}); \rho(\vec{r}) \\ &= \int \frac{d^2\Delta}{(2\pi)^2} F_{2g}(\Delta, x_1) \exp(i\vec{\Delta}\vec{r}), \end{aligned} \tag{5}$$

where $\rho(\vec{r})$ is the transverse parton density. Note that in such approach the parton density is normalized by one

$$\int \rho(\vec{r}) d^2 r = 1. \tag{6}$$

The effective cross section is then given by

$$\frac{1}{\sigma_{\text{eff}}} = \int d^2 b (\int d^2 r \rho(\vec{r}) \rho(\vec{r} - \vec{b}))^2, \tag{7}$$

where $\vec{b}$ is the impact parameter of the proton proton collision.

3 The hot spots model

The hot spots mode assumes a specific type of distribution for the transverse positions of the gluonic content of the proton [6,7]. According to the model the gluons are concentrated around N_q points, called the hot spots, positioned in the transverse positions $\vec{b}_i$ with a two-dimensional Gaussian distribution around the center of mass the proton, marked as $\vec{c}$, with the width B_p. The hot spots distribution around a known center is:

$$\begin{aligned} \rho\left(\left\{\vec{b}_i\right\}_{i=1}^{N_q} | \vec{c}\right) = \frac{2\pi B_p}{N_q} \delta^{(2)}\left(\frac{\sum_{i=1}^{N_q} \vec{b}_i}{N_q} - \vec{c}\right) \\ \times \left(\prod_{i=1}^{N_q} \frac{1}{2\pi B_p} e^{-\frac{(\vec{b}_i - \vec{c})^2}{2B_p}}\right), \end{aligned} \tag{8}$$

where the normalization factor of $2\pi B_p/N_q$ is chosen to get a total integral of one. Each hot spot has the Gaussian density around the center of the hot spot with a width of B_q and can have a fluctuating strength denote as p_i. Hence, the probability distribution to have a hard parton at position $\vec{r}$ is given by:

$$\begin{aligned} \rho\left(\vec{r}, \left\{\vec{b}_i, p_i\right\}_{i=1}^{N_q} | \vec{c}\right) = \frac{2\pi B_p}{N_q} \delta^{(2)}\left(\frac{\sum_{i=1}^{N_q} \vec{b}_i}{N_q} - \vec{c}\right) \\ \times \left(\prod_{i=1}^{N_q} \frac{1}{2\pi B_p} e^{-\frac{(b_i - \vec{c})^2}{2B_p}}\right) \\ \times \left(\frac{1}{N_q} \sum_{i=1}^{N_q} p_i \frac{1}{2\pi B_q} e^{-\frac{(\vec{r} - \vec{b}_i)^2}{2B_q}}\right). \end{aligned} \tag{9}$$

Here the hot spot strengths p_i are assumed to have random distribution

$$P(\log(p_i)) = \frac{1}{\sqrt{2\pi}\sigma} \exp(-\log(p_i)^2/2\sigma^2), \tag{10}$$

so that $\bar{p}_i \equiv E(p_i)$-average value of p_i is equal to $\exp(\sigma^2/2)$, and overall normalisation is chosen to ensure normalization condition 6.

Using the distribution 10 we obtain for the average value of p^n $E(p^n)$

$$E\left[p^n\right] = e^{\frac{n^2\sigma^2}{2}}. \tag{11}$$

Note that if we take into account the fluctuating strength in order to satisfy the normalization condition (6) we would have to divide the average density by factor $E(p)$ and the product of four densities that appears in the formula for the cross section by

$$E\left[p\right]^4 = e^{2\sigma^2}. \tag{12}$$

4 Calculating the DPS effective cross-section

In order to calculate the effective cross section we need to calculate the event by event cross section for given positions of hot spots and impact parameter $\vec{b}$, and the hot spot strengths using Eq. 7, and then average over the hot spot positions, impact parameter and hot spot strengths. The average of the hot spots positions is done by taking an integral over the positions of the hot-spots, marked as $\left\{\vec{a}_i, \vec{b}_j\right\}_{i,j=1}^{N_q}$ in addition to the collision impact parameter $\vec{b}$. Next we shall average over the hot spot strength fluctuations using Eqs. 10, 11, and 12.

We start by finding the convolution of the single hot spot collision, obtaining the following integral:

$$\begin{aligned}
&\int d^2r\rho\left(\vec{r}, \{\vec{a}_i\}_{i=1}^{N_q}, \vec{c}\right)\rho\left(\vec{r}, \left\{\vec{b}_j\right\}_{j=1}^{N_q}, \vec{c}+\vec{b}\right) \\
&\quad\propto \sum_{i,j}\int d^2r e^{-\frac{(\vec{r}-\vec{a}_i)^2+(\vec{r}-\vec{b}_j)^2}{2B_q}} \\
&\quad= \pi B_q \sum_{i,j} e^{-\frac{(\vec{a}_i-\vec{b}_j)^2}{4B_q}}.
\end{aligned} \tag{13}$$

This integral is proportional to the probability for a single hard partonic process to occur for general positions of the hot spots. Taking the square of this expression and integrating it over the hot spots positions to find $(\sigma_{\text{eff}})^{-1}$. To do that we need to separate the sums into three different classes. If the positions of the hot spots are marked as $\vec{a}_{i_1}$, $\vec{a}_{i_2}$, $\vec{b}_{j_1}$ and $\vec{b}_{j_2}$ we write the classes as (Fig. 2).

- Class I: The two partons come from one hot spot for both protons, or $i_1 = i_2$ and $j_1 = j_2$.
- Class II: One proton emits the two partons from a single hot spot while the other emits them from two different hot-spots, or $i_1 = i_2$ and $j_1 \neq j_2$ or $i_1 \neq i_2$ and $j_1 = j_2$.

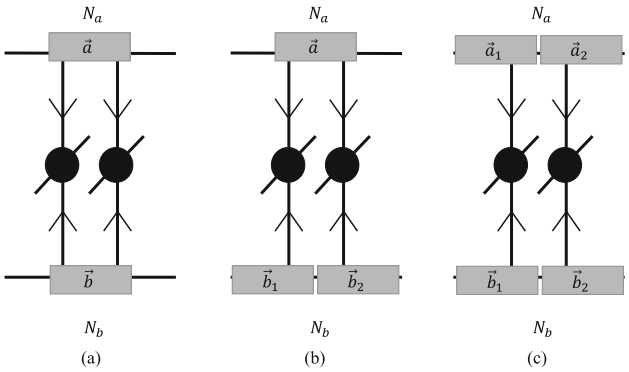

Fig. 2 Three distinct classes of diagrams for DPS scattering in the hot spots model

- Class III: Each proton emits the two partons from different hot spots, or $i_1 \neq i_2$ and $j_1 \neq j_2$.

In addition to separating the sums into cases we also use change the delta function to a form more convenient in the present calculation:

$$\begin{aligned}
&\delta^{(2)}\left(\frac{\sum_{i=1}^{N_q}\vec{a}_i}{N_q} - \vec{c}\right)\delta^{(2)}\left(\frac{\sum_{j=1}^{N_q}\vec{b}_j}{N_q} - \left(\vec{c}+\vec{b}\right)\right) \\
&= \int \frac{d^2s_1 d^2s_2}{(2\pi)^4} e^{i\vec{s}_1\cdot\left(\frac{\sum_{i=1}^{N_q}\vec{a}_i}{N_q}-\vec{c}\right)} e^{i\vec{s}_2\cdot\left(\frac{\sum_{j=1}^{N_q}\vec{b}_j}{N_q}-\left(\vec{c}+\vec{b}\right)\right)}
\end{aligned} \tag{14}$$

We also need the integral over a hot spot that isn't part of the collision, it is simply:

$$\begin{aligned}
I\left(\vec{c}, \vec{s}\right) &\equiv \int d^2b_j e^{\frac{i}{N_q}\vec{s}\cdot\vec{b}_j - \frac{\left(\vec{b}_j-\vec{c}\right)^2}{2B_p}} \\
&= 2\pi B_p e^{-\frac{B_p}{2N_q^2}s^2 + i\frac{1}{N_q}\vec{s}\cdot\vec{c}},
\end{aligned} \tag{15}$$

and the total constant factor is $\left((2\pi)^2 N_q^2 \left(2\pi B_p\right)^{N_q-1}\left(2\pi B_q\right)\right)^{-2}$, we also set the center of the first proton to be $\vec{c} = \vec{0}$ and the second is then $\vec{c} + \vec{b} = \vec{b}$.

4.1 Two partons from a single hot spot of each proton

In case I the two sums become:

$$\begin{aligned}
&\left(\sum_{i_1,j_1} p_{i_1}\tilde{p}_{j_1} e^{-\frac{\left(\vec{a}_{i_1}-\vec{b}_{j_1}\right)^2}{4B_q}}\right)\left(\sum_{i_2,j_2} p_{i_2}\tilde{p}_{j_2} e^{-\frac{\left(\vec{a}_{i_2}-\vec{b}_{j_2}\right)^2}{4B_q}}\right) \\
&\quad\to p^2\tilde{p}^2 {N_q}^2 e^{-\frac{\left(\vec{a}_1-\vec{b}_1\right)^2}{2B_q}},
\end{aligned} \tag{16}$$

where we get a factor of N_q^2 from choosing a single hot spot in each proton without loss of generality and $\tilde{p}$ represent the

hot spot strength from the b proton. The $2N_q - 2$ hot spots in two nucleons that are not involved in the interaction give us a factor of $\left(I\left(\vec{0},\vec{s}_1\right) I\left(\vec{b},\vec{s}_2\right)\right)^{N_q-1}$. We are left with the following integral:

$$A = \frac{p^2\tilde{p}^2}{4N_q^4\left(2\pi\right)^6 B_q^2}\int d^2b d^2s_1 d^2s_2 d^2a_1 d^2b_1 \times e^{-\frac{(N_q-1)B_p}{2N_q^2}\left(s_1^2+s_2^2\right)-i\frac{1}{N_q}\vec{s}_2\cdot\vec{B}-\frac{\left(\vec{a}_1-\vec{b}_1\right)^2}{2B_q}+\frac{i}{N_q}\left[\vec{s}_1\cdot\vec{a}_1+\vec{s}_2\cdot\vec{b}_1\right]-\frac{a^2+\left(\vec{b}_1-\vec{b}\right)^2}{2B_p}}. \tag{17}$$

We are left with a 10-dimensional Gaussian, but really, the two Cartesian coordinates are completely separable so really we can write integral A as the square of a 5-dimensional Gaussian. If we write the parameters as a vector $\vec{x}^T = (a_{1x}, b_{1x}, b_x, s_{1x}, s_{2x})$ we obtain:

$$A = \frac{p^2\tilde{p}^2}{4N_q^4\left(2\pi\right)^6 B_q^2}\left(\int d^5x e^{-\vec{x}^T M_A \vec{x}}\right)^2, \tag{18}$$

with M being the following symmetric matrix:

$$M_A = \begin{pmatrix} \frac{B_p+B_q}{2B_pB_q} & -\frac{1}{2B_q} & 0 & -\frac{i}{2N_q} & 0 \\ -\frac{1}{2B_q} & \frac{B_p+B_q}{2B_pB_q} & -\frac{1}{2B_p} & 0 & -\frac{i}{2N_q} \\ 0 & -\frac{1}{2B_p} & \frac{1}{2B_p} & 0 & \frac{i}{2N_q} \\ -\frac{i}{2N_q} & 0 & 0 & \frac{N_q-1}{2N_q^2}B_p & 0 \\ 0 & -\frac{i}{2N_q} & \frac{i}{2N_q} & 0 & \frac{N_q-1}{2N_q^2}B_p \end{pmatrix}, \tag{19}$$

and we can use the Gaussian formula $\int d^n x e^{-\vec{x}^T M\vec{x}} = \frac{(2\pi)^{n/2}}{\sqrt{\det M}}$ to get:

$$A = \frac{p^2\tilde{p}^2}{8\pi B_q {N_q}^2}. \tag{20}$$

Averaging over p and $\tilde{p}$ we obtain:

$$A = \frac{E\left[p^2\right]^2}{8\pi B_q {N_q}^2} = \frac{e^{4\sigma^2}}{8\pi B_q {N_q}^2}. \tag{21}$$

This expression takes into account fluctuations of the hot spot strength. If we neglect the fluctuations of the hot spot strength, which corresponds to setting $\sigma = 0$, we would get:

$$A_{\sigma=0} = \frac{1}{8\pi B_q {N_q}^2}. \tag{22}$$

4.2 Two partons from a single hot spot of one proton and two different hot spots from the other proton

In case II the two sums become one of two sub-cases, for $i_1 = i_2$ but $j_1 \neq j_2$ we get:

$$\left(\sum_{i_1,j_1} p_{i_1}\tilde{p}_{j_1} e^{-\frac{\left(\vec{a}_{i_1}-\vec{b}_{j_1}\right)^2}{4B_q}}\right)\left(\sum_{i_2,j_2} p_{i_2}\tilde{p}_{j_2} e^{-\frac{\left(\vec{a}_{i_2}-\vec{b}_{j_2}\right)^2}{4B_q}}\right) \to p^2\tilde{p}_1\tilde{p}_2 {N_q}^2\left(N_q-1\right) e^{-\frac{\left(\vec{a}_1-\vec{b}_1\right)^2+\left(\vec{a}_1-\vec{b}_2\right)^2}{4B_q}}, \tag{23}$$

where the factor of ${N_q}^2\left(N_q-1\right)$ comes from choosing the hot spots without loss of generality. In this sub-case, we also get a factor of $\left(I\left(\vec{0},\vec{s}_1\right)\right)^{N_q-1}\left(I\left(\vec{b},\vec{s}_2\right)\right)^{N_q-2}$, leaving us with the integral:

$$B_1 = \frac{\left(N_q-1\right)p^2\tilde{p}_1\tilde{p}_2}{2N_q^5\left(2\pi\right)^7 B_p B_q^2}\left(\int d^6x e^{-\vec{x}^T M_{B_1}\vec{x}}\right)^2, \tag{24}$$

where now $\vec{x}^T = (a_{1x}, b_{1x}, b_{2x}, b_x, s_{1x}, s_{2x})$ and:

$$M_{B_1} = \begin{pmatrix} \frac{B_p+B_q}{2B_pB_q} & -\frac{1}{4B_q} & -\frac{1}{4B_q} & 0 & -\frac{i}{2N_q} & 0 \\ -\frac{1}{4B_q} & \frac{B_p+2B_q}{4B_pB_q} & 0 & -\frac{1}{2B_p} & 0 & 0 \\ -\frac{1}{4B_q} & 0 & \frac{B_p+2B_q}{4B_pB_q} & -\frac{1}{2B_p} & 0 & -\frac{i}{2N_q} \\ 0 & -\frac{1}{2B_p} & -\frac{1}{2B_p} & \frac{1}{B_p} & 0 & -\frac{i}{2N_q} \\ -\frac{i}{2N_q} & 0 & 0 & 0 & \frac{N_q-1}{2N_q^2}B_p & \frac{i}{N_q} \\ 0 & 0 & -\frac{i}{2N_q} & -\frac{i}{2N_q} & \frac{i}{N_q} & \frac{N_q-2}{2N_q^2}B_p \end{pmatrix}. \tag{25}$$

Using the Gaussian formula we get

$$B_1 = \frac{\left(N_q-1\right)p^2\tilde{p}_1\tilde{p}_2}{4\pi\left(B_p+2B_q\right)N_q^2}. \tag{26}$$

For the second sub-case, $i_1 \neq i_2$ and $j_1 = j_2$, it can be shown that we get the same constant factor but a different matrix, but overall the determinants are the same so we get $B_2 = B_1 \Rightarrow B = 2B_1$. The average over the hot spots strengths gives the final expression for this case:

$$B = \frac{\left(N_q-1\right)E\left[p^2\right]E\left[p\right]^2}{2\pi\left(B_p+2B_q\right){N_q}^2} = \frac{\left(N_q-1\right)e^{3\sigma^2}}{2\pi\left(B_p+2B_q\right){N_q}^2}, \tag{27}$$

In the case when fluctuations of the hot spot strength are neglected $\sigma = 0$ we obtain:

$$B_{\sigma=0} = \frac{\left(N_q-1\right)}{2\pi\left(B_p+2B_q\right)N_q^2}. \tag{28}$$

4.3 Two different hot spots from both protons

In the case II the two sums become one of two sub-cases. For $i_1 \neq i_2$ but $j_1 \neq j_2$ we get for the sums:

$$\left(\sum_{i_1,j_1} p_{i_1}\tilde{p}_{j_1} e^{-\frac{\left(\vec{a}_{i_1}-\vec{b}_{j_1}\right)^2}{4B_q}}\right)\left(\sum_{i_2,j_2} p_{i_2}\tilde{p}_{j_2} e^{-\frac{\left(\vec{a}_{i_2}-\vec{b}_{j_2}\right)^2}{4B_q}}\right) \to p_1\tilde{p}_1 p_2\tilde{p}_2 N_q^2\left(N_q-1\right)^2 e^{-\frac{\left(\vec{a}_1-\vec{b}_1\right)^2+\left(\vec{a}_2-\vec{b}_2\right)^2}{4B_q}}, \tag{29}$$

Table 1 The four parameters used in our calculations as taken from [6] for the case of Variable N_q and $N_q \equiv 3$

Parameter	Description	Variable N_q	$N_q \equiv 3$
N_q	Number of hot spots	$6.79^{+2.93}_{-4.83}$	3
σ	Magnitude of hot spots strength fluctuations	$0.833^{+0.194}_{-0.441}$	$0.563^{+0.143}_{-0.141}$
$B_q\,[GeV^{-2}]$	Hot spot size	$0.474^{+0.434}_{-0.286}$	$0.346^{+0.282}_{-0.202}$
$B_p\,[GeV^{-2}]$	Proton size	$4.02^{+1.73}_{0.728}$	$4.45^{+0.801}_{-0.803}$

with a factor of $\left(I\left(\vec{0},\vec{s}_1\right)I\left(\vec{b},\vec{s}_2\right)\right)^{N_q-2}$ we get the integral to be:

$$C=\frac{p_1\tilde{p}_1 p_2\tilde{p}_2\left(N_q-1\right)^2}{4N_{q^4}\left(2\pi\right)^8 B_p^2 B_q^2}\left(\int d^7x e^{-\vec{x}^T M_C\vec{x}}\right)^2, \tag{30}$$

with the vectors being $\vec{x}^T=(a_{1x},a_{2x},b_{1x},b_{2x},b_x,s_{1x},s_{2x})$ and the matrix:

$$M_C=\begin{pmatrix}
\frac{B_p+2B_q}{4B_pB_q} & 0 & -\frac{1}{4B_q} & 0 & 0 & -\frac{i}{2N_q} & 0\\
0 & \frac{B_p+2B_q}{4B_pB_q} & 0 & -\frac{1}{4B_q} & 0 & -\frac{i}{2N_q} & 0\\
-\frac{1}{4B_q} & 0 & \frac{B_p+2B_q}{4B_pB_q} & 0 & -\frac{1}{2B_p} & 0 & -\frac{i}{2N_q}\\
0 & -\frac{1}{4B_q} & 0 & \frac{B_p+2B_q}{4B_pB_q} & -\frac{1}{2B_p} & 0 & -\frac{i}{2N_q}\\
0 & 0 & -\frac{1}{2B_p} & -\frac{1}{2B_p} & \frac{1}{B_p} & 0 & \frac{i}{N_q}\\
-\frac{i}{2N_q} & -\frac{i}{2N_q} & 0 & 0 & 0 & \frac{N_q-2}{2N_q^2}B_p & 0\\
0 & 0 & -\frac{i}{2N_q} & -\frac{i}{2N_q} & \frac{i}{N_q} & 0 & \frac{N_q-2}{2N_q^2}B_p
\end{pmatrix}. \tag{31}$$

Using the Gaussian formula we get:

$$C=\frac{p_1\tilde{p}_1 p_2\tilde{p}_2\left(N_q-1\right)^2}{8\pi\left(B_p+B_q\right)N_q^2}, \tag{32}$$

average over the hot spots strength gives us the final form for this case:

$$C=\frac{E\left[p\right]^4\left(N_q-1\right)^2}{8\pi\left(B_p+B_q\right)N_q^2}=\frac{\left(N_q-1\right)^2 e^{2\sigma^2}}{8\pi\left(B_p+B_q\right)N_q^2}, \tag{33}$$

If the fluctuations of the hot spot strength are neglected, $\sigma=0$ and we obtain

$$C_{\sigma=0}=\frac{\left(N_q-1\right)^2}{8\pi\left(B_p+B_q\right)N_q^2}. \tag{34}$$

5 Total effective cross section in hot spot model

Putting together our results in Eqs. 12, 21, 27, and 33 we find $\sigma_{\rm eff}$ to be:

$$\sigma_{\rm eff}=(A+B+C)^{-1}=\frac{8\pi N_q^2}{\frac{e^{2\sigma^2}}{B_q}+\frac{4(N_q-1)e^{\sigma^2}}{B_p+2B_q}+\frac{(N_q-1)^2}{B_p+B_q}}. \tag{35}$$

Here we normalized the gluon density to one according Eq. 6 using Eq. 12.

Using the parameters from Table I in [6], which for convenience we present here as Table 1, we get two possible values for $\sigma_{\rm eff}$:

$$\begin{aligned}
&\sigma_{\rm eff}\approx 17\ \text{mb}\ \text{ for }\ \text{variable}\ N_q=6.79,\\
&\sigma_{\rm eff}\approx 10.5\ \text{mb for}\ N_q=3.
\end{aligned} \tag{36}$$

Note that in our calculations we use the fit number 6.78 from the table, although of course the actual number of hot spots is integer. We refer to this fit as "variable N_q".

6 Comparison with the DPS experimental data

Let us compare now our results with the experimental data on 4 jet DPS production. Such data exists for both ATLAS and CMS collaborations for jets with transverse momenta $p_T > 20$ GeV. The experimental situation is summarized in Fig. 1 of [26].

One can see that CMS results for 4-jet DPS effective cross section are in the 13 ± 3 mb range for the 2021 measurement [27]. These numbers are in agreement with the latest 2016 ATLAS measurements [25,28], although look different from larger effective cross section 20 ± 5 mb reported earlier by CMS [29]. Note also that both 2016 results were obtained based on analysis of the data at energies: $\sqrt{s}$ equal 7 TeV vs 13 TeV for 2021 results [27].

On the first sight these experimental results are compatible with the hot spot model results (36), although for $N_q=3$ they are on the low boundary of allowed measurements results. However such conclusion does not take into account the pQCD evolution: the hot spot model is formulated at the scales of order 1 GeV (see below) while jet cross sections determined by dynamics at the scales larger than 20 GeV.

The pQCD evolution of $\sigma_{\rm eff}$ was analyzed recently [12–23], see also the recent book of reviews [24]. The main result is that the effective cross section depends on the hard scale of a process. This is due to the so called $1\to2$ processes.

These processes (see Fig. 3) were found to result in a substantial decrease of $\sigma_{\rm eff}$ with increase of momentum scale of the DPS.

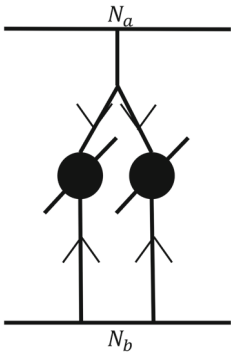

Fig. 3 The $1 \to 2$ mechanism for DPS scattering

Note that the transverse momentum scale of the fit for the hot spots model can be estimated as $\frac{\pi}{2r_{hotspot}} \sim 1$ GeV. The transverse scale of the four jet data is ~ 20 GeV, so one needs to take the QCQ evolution in account, when applying it to multi GeV processes like jet production.

The direct calculation of $1 \to 2$ contributions using [21] shows that the effective cross sections for two scales discussed here are related as

$$\sigma_{\rm eff}(20\ GeV)/\sigma_{\rm eff}(1\ GeV) \sim 0.6. \tag{37}$$

This means that we need to compare the hot spot model results with effective cross sections 20 ± 5 mb for [28] and [27], and 32 ± 8 mb for CMS 2016 (see Table 2). Note that the CMS2016 results for $\sigma_{\rm eff}$ are close to those used in PYTHIA and HERWIG MC generators [32,33]. The values of $\sigma_{\rm eff}$ calculated within the hot spot model are compared with the data in Table 1 for $N_q = 3$ and variable N_q. We observe that there is a significant tension with the hot spot model results especially for $N_q = 3$. However more experimental data is needed to reach definite conclusions.

7 Conclusions

In this paper we calculated the effective DPS cross section for hot spot models. We see that potentially the DPS experimental data provides a strong constraint on these models. For current data we see that there are some signs of tension with the hot spot model fits, although more experimental data and more fit details such as uncertainties in parameters of the fits are necessary to reach more definite conclusions.

Table 2 The results of $\sigma_{\rm eff}$ measurements and their hard scale dependence versus hot spot model fits

Measurement	$\sigma_{\rm eff}$ at scale 20 GeV	$\sigma_{\rm eff}$ at scale $\sim$1 GeV
CMS 2021 [27] and ATLAS 2016 [28]	13 ± 3 mb	20 ± 5 mb
CMS2016 [29]	20 ± 5 mb	32 ± 8 mb
Hot spots fit $N_q = 3$		~ 10 mb
Hot spots fit variable N_q		~ 17 mb

Acknowledgements The research of B. Blok and R. Segev was supported by ISF grant number 2025311 and BSF grant 2020115. The research of M. Strikman was supported by BSF grant 2020115 and by US Department of Energy Office of Science, Office of Nuclear Physics under Award No. DE-FG02-93ER40771.

Data Availability Statement This manuscript has no associated data or the data will not be deposited. [Authors' comment: This paper is a theoretical work. No experimental data were used.]

Funded by SCOAP^3. SCOAP^3 supports the goals of the International Year of Basic Sciences for Sustainable Development.

References

1. R. Abdul Khalek et. al., Science requirements and detector concepts for the electron-ion collider: EIC Yellow Report. arXiv:2103.05419 [physics.ins-det]
2. B. Blok, M. Strikman, Adv. Ser. Direct High Energy Phys. **29**, 63–99 (2018). [arXiv:1709.00334 [hep-ph]]
3. E.M. Levin, L.L. Frankfurt, UFN **94**, 243–288 (1968) [Sov. Phys. Usp. **11**, 106–129 (1968)]
4. A.H. Mueller, Nucl. Phys. B Proc. Suppl. **18**, 125–132 (1991)
5. H. Mäntysaari, B. Schenke, Phys. Lett. B **772**, 832–838 (2017). arXiv:1703.09256 [hep-ph]
6. H. Mäntysaari, B. Schenke, C. Shen, W. Zhao, Phys. Lett. B **833**, 137348 (2022)
7. H. Mäntysaari, F. Salazar, B. Schenke, Phys. Rev. D **106**(7), 074019 (2022). arXiv:2207.03712 [hep-ph]
8. M.L. Good, W.D. Walker, Phys. Rev. **120**, 1857–1860 (1960)
9. L. Frankfurt, V. Guzey, A. Stasto, M. Strikman, Rep. Prog. Phys. **85**(12), 126301 (2022). arXiv:2203.12289 [hep-ph]
10. N. Paver, D. Treleani, Z. Phys. C **28**, 187 (1985)
11. M. Mekhfi, Phys. Rev. D **32**, 2371 (1985)
12. J.R. Gaunt, W.J. Stirling, JHEP **1003**, 005 (2010). [arXiv:0910.4347 [hep-ph]]
13. B. Blok, Yu. Dokshitzer, L. Frankfurt, M. Strikman, Phys. Rev. D **83**, 071501 (2011). [arXiv:1009.2714 [hep-ph]]
14. M. Diehl, PoS D **IS2010**, 223 (2010). arXiv:1007.5477 [hep-ph]
15. J.R. Gaunt, W.J. Stirling, JHEP **1106**, 048 (2011). [arXiv:1103.1888 [hep-ph]]
16. B. Blok, Yu. Dokshitser, L. Frankfurt, M. Strikman, Eur. Phys. J. C **72**, 1963 (2012). [arXiv:1106.5533 [hep-ph]]
17. M. Diehl, D. Ostermeier, A. Schafer, JHEP **1203**, 089 (2012). [arXiv:1111.0910 [hep-ph]]

18. B. Blok, Y. Dokshitzer, L. Frankfurt, M. Strikman, Eur. Phys. J. C **74**, 2926 (2014). [arXiv:1306.3763 [hep-ph]]
19. M. Diehl, J.R. Gaunt, K. Schönwald, JHEP **1706**, 083 (2017). [arXiv:1702.06486 [hep-ph]]
20. A.V. Manohar, W.J. Waalewijn, Phys. Rev. D **85**, 114009 (2012)
21. B. Blok, P. Gunnellini, Eur. Phys. J. C **75**(6), 282 (2015). https://doi.org/10.1140/epjc/s10052-015-3520-8. arXiv:1503.08246 [hep-ph]
22. J.R. Gaunt, R. Maciula, A. Szczurek, Phys. Rev. D **90**(5), 054017 (2014). https://doi.org/10.1103/PhysRevD.90.054017. arXiv:1407.5821 [hep-ph]
23. K. Golec-Biernat, E. Lewandowska, Phys. Rev. D **90**(9), 094032 (2014). https://doi.org/10.1103/PhysRevD.90.094032. arXiv:1407.4038 [hep-ph]
24. P. Bartalini, J.R. Gaunt, Adv. Ser. Direct High Energy Phys. **29**, 1–450 (2018). https://doi.org/10.1142/10646
25. O. Kuprash [ATLAS], Studies of the underlying-event properties and of hard double parton scattering with the ATLAS detector. PoS **DIS2017**, 035 (2018)
26. R. Gupta [CMS and TOTEM], Double parton scattering studies in CMS. PoS **EPS-HEP2021**, 335 (2022)
27. A. Tumasyan et al. [CMS], JHEP **01**, 177 (2022). https://doi.org/10.1007/JHEP01(2022)177. arXiv:2109.13822 [hep-ex]
28. M. Aaboud et al. [ATLAS], JHEP **11**, 110 (2016). https://doi.org/10.1007/JHEP11(2016)110. arXiv:1608.01857 [hep-ex]
29. R. Kumar et al. [CMS], Springer Proc. Phys. **203**, 529–531 (2018). https://doi.org/10.1007/978-3-319-73171-1_124
30. M. Diehl, Phys. Rep. **388**, 41–277 (2003). arXiv:hep-ph/0307382
31. A.V. Belitsky, A.V. Radyushkin, Phys. Rep. **418**, 1–387 (2005). arXiv:hep-ph/050400
32. T. Sjöstrand, Adv. Ser. Direct High Energy Phys. **29**, 191–225 (2018). arXiv:1706.02166 [hep-ph]
33. J. Bellm, S. Gieseke, P. Kirchgaesser, Eur. Phys. J. C **80**(5), 469 (2020). arXiv:1911.13149 [hep-ph]